

SEMI-ANNUAL STATUS REPORT  
NASA AMES GRANT NGR 37-008-003  
FOR THE PERIOD JANUARY TO JUNE 1974

(NASA-CR-139407) ENERGY TRANSFER IN  
VOLUME-REFLECTING HEAT SHIELDS Semiannual  
Status Report, Jan. - Jun. 1974 (Tulsa  
Univ.) 19 p HC \$4.00 CACL 20M

N74-30369

Unclas

G3/33 54914

ENERGY TRANSFER IN VOLUME-REFLECTING HEAT SHIELDS

University of Tulsa  
Department of Mechanical Engineering  
Tulsa, Oklahoma 74104

Dr. Kenneth C. Weston  
Principal Investigator

## STATUS REPORT - JUNE 1974

NASA AMES GRANT NGR 37-008-003\*

During the subject reporting period the research discussed herein was advanced by a graduating mechanical engineering senior, Daniel W. Drago, and the principal investigator. As a consequence of the previously unprogrammed investigation of some interesting aspects of radiative transfer calculations for non-unity index of refraction (discussed below), a request for extension of the completion date of the present research to August 31, 1974 was requested and recently approved. Mr. Drago is remaining at the University as a graduate student and will be participating through the grant termination date.

In the present reporting period two papers have been submitted for publication and another paper published. As reported in the last status report, a paper by R. S. Reddy and the principal investigator had been submitted to and accepted for publication by the AIAA Journal. This paper, which has since appeared in the Journal (reference 1), provides an approximate analytic solution for the unsteady radiative heating of a highly scattering medium under constant heat flux boundary conditions.

A more recent paper prepared under this grant (reference 2) explores the accuracy of two-flux methods (such as that employed in reference 1) in representing the reflectance, radiative flux and radiative flux divergence of highly scattering materials. The influence of anisotropic scattering on these parameters was also considered. This work, not accepted for presentation at the 1974 Heat Transfer and Fluid Mechanics Institute, has been revised and submitted for publication in the AIAA Journal. In addition to defining conditions of

---

\*The NASA Technical Officer for this grant is Dr. Phillip R. Nachtsheim, NASA Ames Research Center, Moffett Field, CA 94035.

applicability of approximate methods, this work clarifies relations between transfer equation solutions and approximate methods, and presents new results for anisotropic scattering.

Still more recently, while evaluating the capabilities of the NANITERAD program in dealing with radiative transfer in media with non-unity refractive index, solution intensities were found to vary erratically with quadrature order. Through an approximate discontinuity model and transfer equation solutions we have shown that, for a fixed quadrature, the quadrature accuracy (and hence transfer equation solution accuracy) varies erratically with refractive index rather than smoothly as implied in the literature (reference 3 for instance). The discontinuity model shows that under certain conditions the accuracy of Gaussian quadrature may decrease with increasing quadrature order rather than increase as found with continuous distributions. The observed error pattern is due to the relative position of the critical angle for total internal reflection and its neighboring quadrature directions. It was found that the errors induced by the discontinuity are amplified in an iterative solution due to the scattering term in the transfer equation. A published solution (reference 3) for refractive index of 1.4 was shown to exhibit a large discontinuity error as predicted by the model. As a result of this study we are revising our calculation procedures to incorporate separate quadratures within and outside the critical angle for total internal reflection. For a continuous distribution the accuracy of the numerical integration is reduced by using several quadrature formulae in place of a single quadrature application with the same total number of directions. However for the non-unity index cases, this loss may be far exceeded by the gain in accuracy achieved by discontinuity error avoidance. A discussion of the errors incurred by the use of single quadrature has been presented in a paper submitted to the ASME Journal of Heat

Transfer (reference 4). We have been advised that the general reaction of the ASME reviewers was favorable. The paper has been resubmitted incorporating certain revisions as requested.

The formation of a minimum in the magnitude of reflected intensities near the rear surface of an absorbing and scattering slab is considered in Appendix A of this report. The intensities decrease, stabilize and increase as the front surface is approached. This unexpected phenomenon was first considered to occur because of a programming error. A simple analytical distribution model applied to the transfer equation however verified the existence of a dip under certain conditions. Model and transfer equation results are also compared in the Appendix.

A study of the most suitable quadrature formulae combination with a limited number of quadrature directions for non-unity index of refraction has been completed and appears as Appendix B to this status report. This study shows that the most accurate method of formulae application for cases with significant discontinuities uses three separate quadratures over the range  $-1 \leq \mu \leq 1$ , one each within the positive and negative regions of total internal reflection and the third between the other two. The appendix also provides tabulated error results for various single and multiple formulae applications.

The NANITERAD program is at this time regarded as fully operational. A number of cases have shown consistent and reasonable behavior for non-unity refractive index although the results available in the literature for comparison are quite limited. The most convincing check was with a fifth order quadrature calculation given in reference 4. The detailed radiation field agreed with the NANITERAD calculations within reading errors dictated by the small size of the figure of the reference.

## REFERENCES

1. Weston, Kenneth C. and Reddy, R. S., "Unsteady Temperature Distribution in Volume Reflectors," AIAA Journal, Volume 12, No. 9, May 1974, pp. 716-718
2. Weston, Kenneth C., Reynolds, Albert C., Alikhan, Arif and Drago, Daniel W., "Radiative Transfer in Highly Scattering Materials - Numerical Solution and Evaluation of Approximate Analytic Solutions." Submitted for publication in the AIAA Journal.
3. Roux, J. A., Smith, A. M. and Shahrokhi, F., "Effect of Boundary Conditions on the Radiative Reflectance of Dielectric Coatings," AIAA paper 73-148, January 1973.
4. Weston, Kenneth C. and Drago, Daniel W., "Discontinuities in Radiative Transfer Analysis Using Quadrature Formulae." Submitted for publication in the Transactions of the ASME, Journal of Heat Transfer on May 1, 1974.

## APPENDIX A

## THE CONDITIONS FOR INTENSITY EXTREMA

While exploring various aspects of the transfer equation results, the radiative intensities reflected from the rear surface were thought to monotonically increase or decrease towards the front surface. Occasionally the reflected intensities were found to decrease near the rear boundary, stabilize, and increase as the front boundary is approached, forming a distinctive dip. A simple model of the transmitted and reflected intensities is applied to the transfer equation, identifying conditions which allow the minimum intensity to exist between the boundaries.

The intensities at any distance  $y$  from the front surface are modeled as:

$$I(\mu, y) = \begin{cases} I^-(y), & \mu < 0 \\ I^+(y), & \mu > 0 \end{cases} \quad (\text{A1})$$

where  $I^+(y)$  is the transmitted intensity and  $I^-(y)$  the reflected intensity.

By using (A1) in the transfer equation while neglecting the emission term, and considering the variation of  $I^-(y)$  in the direction corresponding to  $-|\mu^*|$  the slope of  $I^-(y)$  becomes (for  $|\mu^*| \neq 0$ ):

$$\frac{dI^-(y)}{dy} = \frac{I^+(y)}{|\mu^*|} \left[ \frac{I^-(y)}{I^+(y)} \left( K + \frac{S}{2} \right) - \frac{S}{2} \right]. \quad (\text{A2})$$

As a special case, with pure absorption (A2) reduces to:

$$\frac{dI^-(y)}{dy} = \frac{K I^-(y)}{|\mu^*|}. \quad (\text{A3})$$

In this case the minimum occurs at the front surface since the slope is always positive or zero.

In a second special case, with pure scattering (A2) yields:

$$\frac{dI^-(y)}{dy} = -\frac{I^+(y)}{|\mu^*|} \left(\frac{S}{2}\right) \left[1 - \frac{I^-(y)}{I^+(y)}\right]. \quad (\text{A4})$$

Since the right hand side of A4) is always negative or zero for a flux incident at  $y = 0$ , the minimum of  $I^-(y)$  is at the rear boundary. Thus in either the pure absorption or pure scattering case the dip may not occur.

For non-vanishing scattering and absorption coefficients an extremum of  $I^-(y)$  occurs when the right side of (A2) vanishes at some point within the medium. At that point (A2) indicates a condition for an extremum to be:

$$\frac{I^-(y)}{I^+(y)} = \frac{1}{2 \frac{K}{S} + 1}. \quad (\text{A5})$$

It may be shown using (A2) and a similar equation for the slope of  $I^+(y)$  that the second derivative of  $I^-(y)$  is always positive or zero:

$$\begin{aligned} |\mu^*|^2 \frac{d^2 I^-(y)}{dy^2} &= \frac{dI^-(y)}{dy} \left(K + \frac{S}{2}\right) - \frac{dI^+(y)}{dy} \left(\frac{S}{2}\right) \\ &= \left[ I^-(y) \left(K + \frac{S}{2}\right) - I^+(y) \left(\frac{S}{2}\right) \right] \left(K + \frac{S}{2}\right) \\ &\quad - \left[ -I^+(y) \left(K + \frac{S}{2}\right) + I^-(y) \left(\frac{S}{2}\right) \right] \left(\frac{S}{2}\right) \\ \text{or} \quad \frac{d^2 I^-(y)}{dy^2} &= \frac{I^-(y) (K^2 + K S)}{|\mu^*|^2} \end{aligned} \quad (\text{A6})$$

Since the right side of (A6) is always non-negative, this precludes the possibility of an extremum being a maximum rather than a minimum. Therefore, if the slope of  $I^-(y)$  at the rear boundary ( $y = y_0$ ) is shown to be negative or zero, a dip will not occur. This slope at the rear surface may be calculated to determine the conditions necessary for the slope to be positive, and thus to provide a third condition for the formation of the dip.

The intensities at the rear surface are modeled as:

$$I(\mu, y_0) = \begin{cases} R_B I^+(y_0) , & \mu < 0 \\ I^+(y_0) , & \mu > 0 \end{cases} \quad (\text{A7})$$

where  $R_B$  is the rear surface reflectivity.

Evaluating (A2) at  $y_0$  using (A7) produces the slope of  $I^-(y_0)$ :

$$\frac{d I^-(y_0)}{dy} = \frac{I^+(y_0)}{|\mu^*|} \left[ R_B \left( K + \frac{S}{2} \right) - \frac{S}{2} \right] . \quad (\text{A8})$$

A positive slope of  $I^-(y_0)$  exists when:

$$R_B > \frac{1}{2 \frac{K}{S} + 1} . \quad (\text{A9})$$

Thus for the model given by (A1) and (A7), three conditions must be satisfied for a dip to exist: non-zero scattering and absorption coefficients; a sufficiently large  $R_B$  consistent with (A9); and a small  $I^-(y)$  consistent with (A5). The latter condition is satisfied only when the optical thickness is large enough for  $I^-(y)$  to obtain its minimum within the boundaries.

The criterion for a minimum from (A9) is evaluated using transfer equation solutions in Figure A1. This figure shows the conditions under which minima were found in the solutions. Due to the deviation of the actual intensity field at the rear surface from that modeled in (A1), the condition for a dip based on (A9) has been compared to transfer equation solutions demonstrating a dip in a majority of the quadrature directions. The data from the solutions has been divided into three categories: 1) None of the eight Gaussian quadrature directions contain a dip; 2) At least one direction displays the minimum; and 3) Five or more directions have a dip. As seen in Figure A1, the minimum  $R_B$

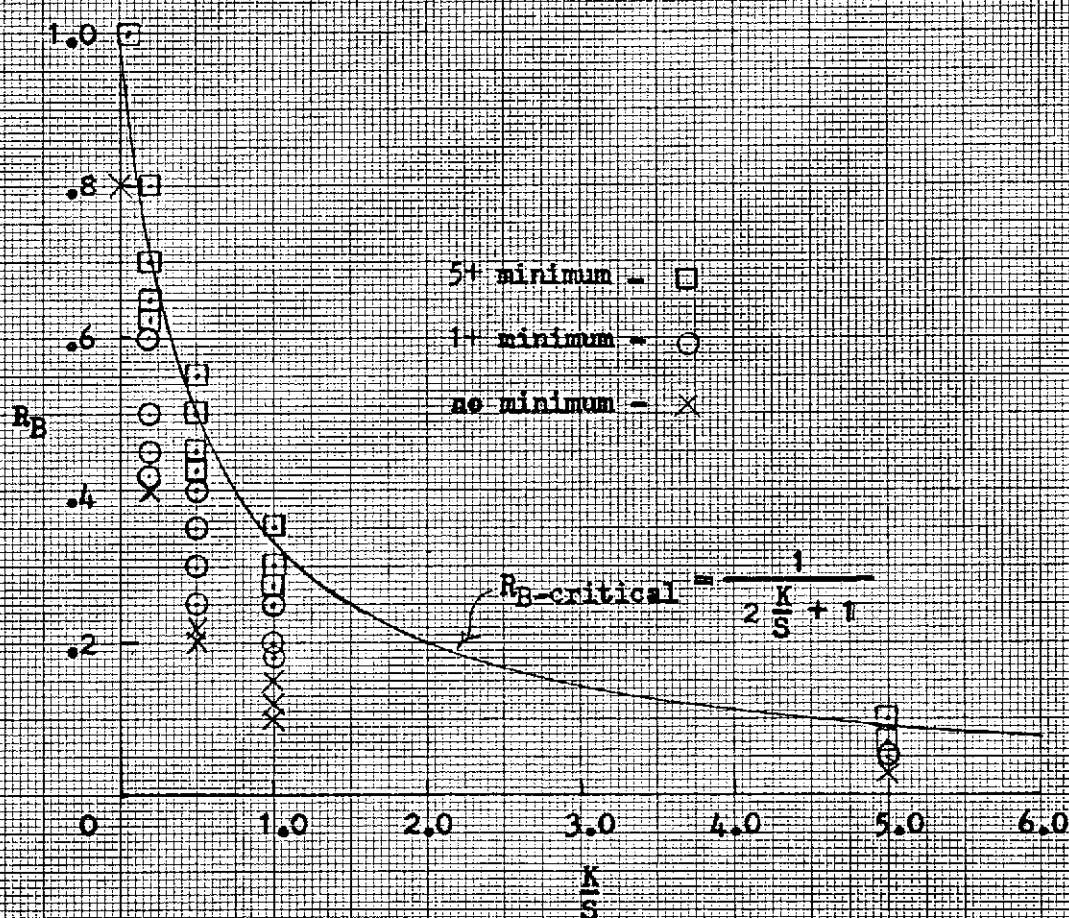


necessary to produce dips in five directions closely follows the trend of the pattern set by condition (A9).

In Figure A2 the optical depth,  $\tau$ , of the minimum from the rear surface is clearly seen to be a function of  $\mu$ . A similar pattern of minima is evident for each case studied. This pattern may be qualitatively explained by referring to equations (A2) and (A6). Assuming a directionally independent value for the reflected beams at the rear boundary and an actual  $R_B$  larger than the  $R_{B-critical}$  from (A9), equation (A2) indicates the reflected beams diminish most rapidly parallel to the boundary. Equation (A6) is even more dependent on  $\mu$  than (A2) due to its inverse relationship to  $\mu^2$ . As such, a plot of the intensity of a beam directed close to parallel to the boundary would demonstrate much larger curvature, and hence would stabilize and begin to increase within substantially less distance from the rear surface, than a beam more nearly normal to the boundary.

A second observation from Figure A2 is that the depth of the minimum from the rear surface in each Gaussian direction generally increases as the ratio of the actual  $R_B$  to the model  $R_{B-critical}$  increases, a pattern further explored in Figure A3. Here the depth of the minimum in the direction closest to normal to the boundaries of the medium is plotted against the ratio of the  $R_B$ 's. The distance of the minimum from the rear surface,  $\tau$ , rapidly increases as the rear surface reflectivity is increased. Lines with constant values of  $k/s$  have generally increasing slope as the value of  $k/s$  decreases, with the smallest plotted value of  $k/s$  producing a nearly vertical line. The actual intensity field becomes more closely approximated by the model in (A1) as  $k/s$  approaches zero, and as such increases the accuracy of prediction based on (A9). Thus, this study shows that minima should be expected to occur over a wide range of conditions for highly scattering media.

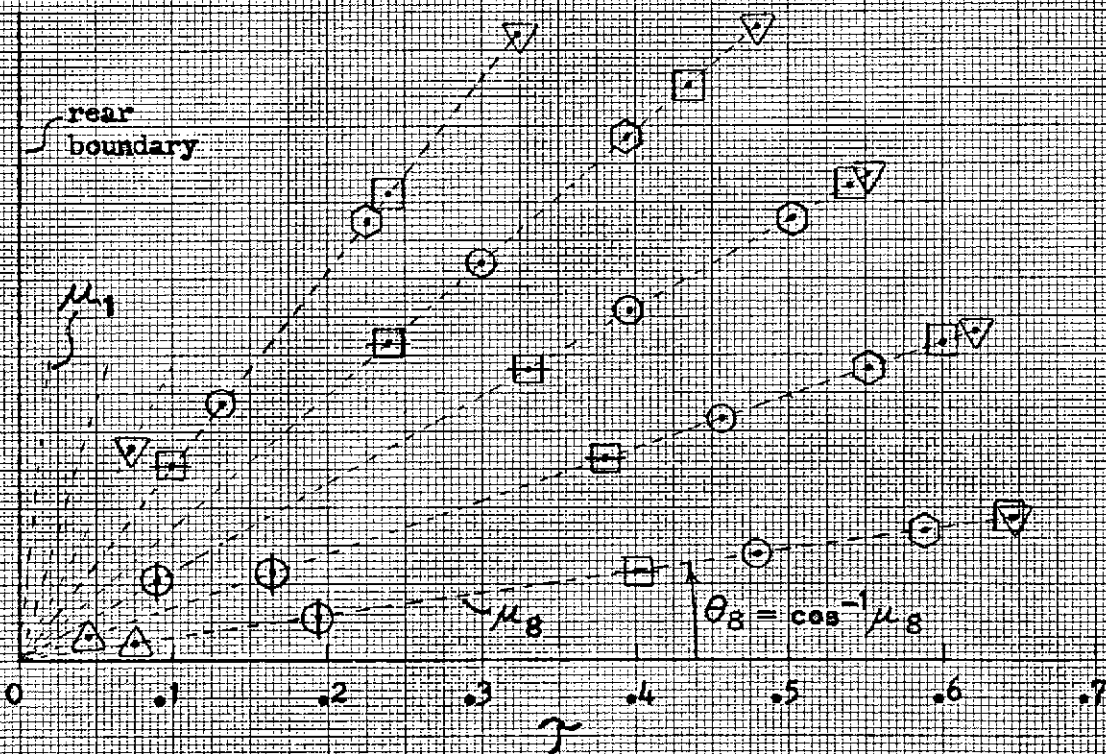
# FIGURE A1



Comparison of the Predicted Critical  $R_B$   
 With the Actual Occurance of the Minimum,  
 Index = 1.0, 0° K, Isotropic Scattering

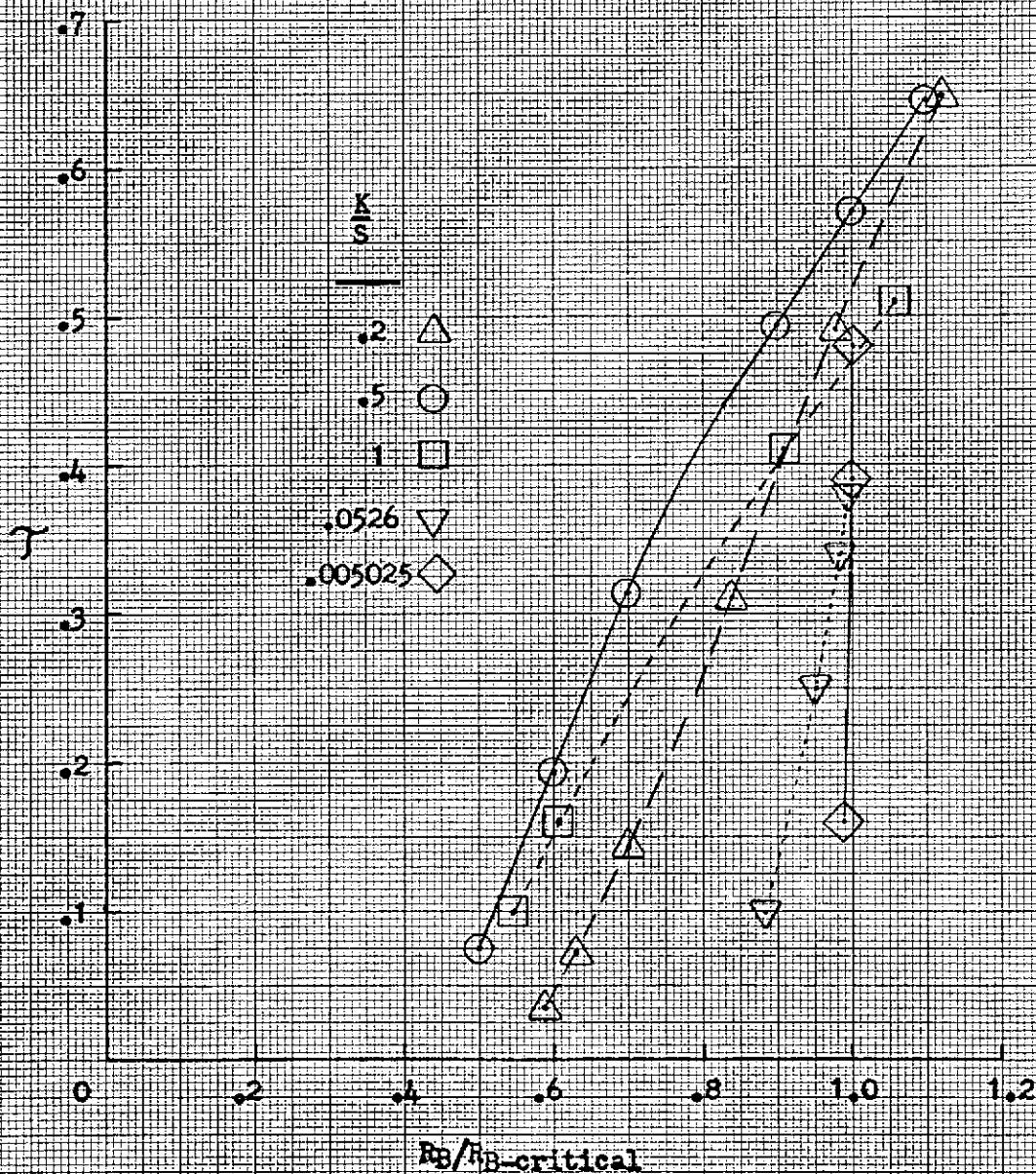
# FIGURE A2

$\frac{K}{S}$	$R_B/R_{B-critical}$	
.2	1.12	▽
.5	1.1	□
5	1.111	○
.2	.98	○
1	.9	□
.5	.6	○
.5	.5	△



Position of the Minimum from the Rear Surface  
 as a Function of  $\mu_s$ ; Index = 1.0,  $0^\circ$  K, Isotropic  
 Scattering

FIGURE A3



Position of the Minimum from the Rear Surface  
 in  $I^{-}(8)$  [near perpendicular to the boundaries];  
 Index = 1.0,  $0^\circ$  K, Isotropic Scattering

## APPENDIX B

## THE ACCURACY OF GAUSSIAN QUADRATURE COMBINATIONS

As discussed in [4], a significant error may be generated in the numerical approximation of the scattering integral in the transfer equation when a single quadrature is used for media with refractive indices greater than one. The error arises from the presence of a discontinuity in the intensity field at the critical angle for total internal reflection due to a Fresnel boundary. Figure B1 shows the computed values of transmission across such a boundary when the quadrature is applied over three different regions. The first and second applications, which are indifferent to the presence of the discontinuity, result in large and erratic errors for small to medium quadrature orders. The third application restricted to the region of transmitted flux only, demonstrates high accuracy even for low quadrature order and smoothly converges to the exact value.

The overall accuracy in the transfer equation solutions when using single quadrature applications has been shown to follow a similar pattern to that found with the first two applications used in Figure B1 [4]. In this appendix the question of which combination of Gaussian quadratures is most suitable for radiative transfer calculations involving discontinuities at the critical angle is considered, with the overall medium reflectance providing a measure of combination quality. The quadrature combinations are applied such that the quadratures selected are bounded by the critical angle and have a combined total of no more than sixteen quadrature points. Three regions of  $\mu$  were defined for the application of quadrature formulae to the scattering integral:

$$\text{Region I: } -1 \leq \mu < -\mu_c$$

$$\text{Region II: } -\mu_c < \mu < \mu_c \quad (\text{B1})$$

$$\text{Region III: } \mu_c < \mu \leq 1$$

where  $\mu_c$  is the cosine of the critical angle of total internal reflection:

$$\mu_c = \sqrt{1 - \left(\frac{1}{N}\right)^2} \quad (\text{B2})$$

and  $N$  the refractive index of the medium. Typically, identical quadrature orders were applied to Regions I and III, with Region II utilizing the remainder of the sixteen quadrature directions.

The notation used here for the quadrature formulae application is:

$$X/Y/X \quad (\text{B3})$$

where  $X$  is the quadrature order of Regions I and III, and  $Y$  is the order of Region II. For example, fourth order quadratures may be used in Regions I and III with eighth in Region II, as expressed by 4/8/4.

Reflectance results for various quadrature combinations used in approximating the transfer equation scattering integral are presented in Table B1. Selected combinations were run for two refractive indices to insure that the relative magnitudes of the reflectance values were not significantly affected by a refractive index change. The same reflectance pattern did appear in both cases, with 5/3/3/5 (Region II was divided at  $\mu = 0$  with two quadratures applied) and 4/8/4 nearly identical, 6/4/6 lower, and 5/6/5 between. As predicted in [4], tenth quadrature was found to have a large error at  $N = 1.4$  while sixteenth was relatively accurate.

As shown in Figures B2 and B3, a reference reflectivity was determined from three sequenced test values found for each refractive index case. These values came from quadrature combinations of 2/4/2, 3/6/3, and 4/8/4, with the values of reflectivity

plotted as a function of the inverse number of total quadrature directions. The reference value was found by extrapolating a line faired on the three test points to the zero value of the abscissa.

Study of these figures and the Table show that both 5/6/5 and 5/3/3/5 are within .12% of the reference values at both refractive indices, with the average percentage error smallest for the 5/6/5 combination. Thus the 5/6/5 application was ultimately selected for use in the transfer equation solutions for cases with non-unity index of refraction. A single quadrature application of sixteenth order was retained for the  $N = 1.0$  cases.

TABLE B1

TABLE OF REFLECTANCE VALUES AND ERRORS  
FOR SEVERAL QUADRATURE COMBINATIONS

$$\omega = 1.0 \quad 0^\circ \text{ K}$$

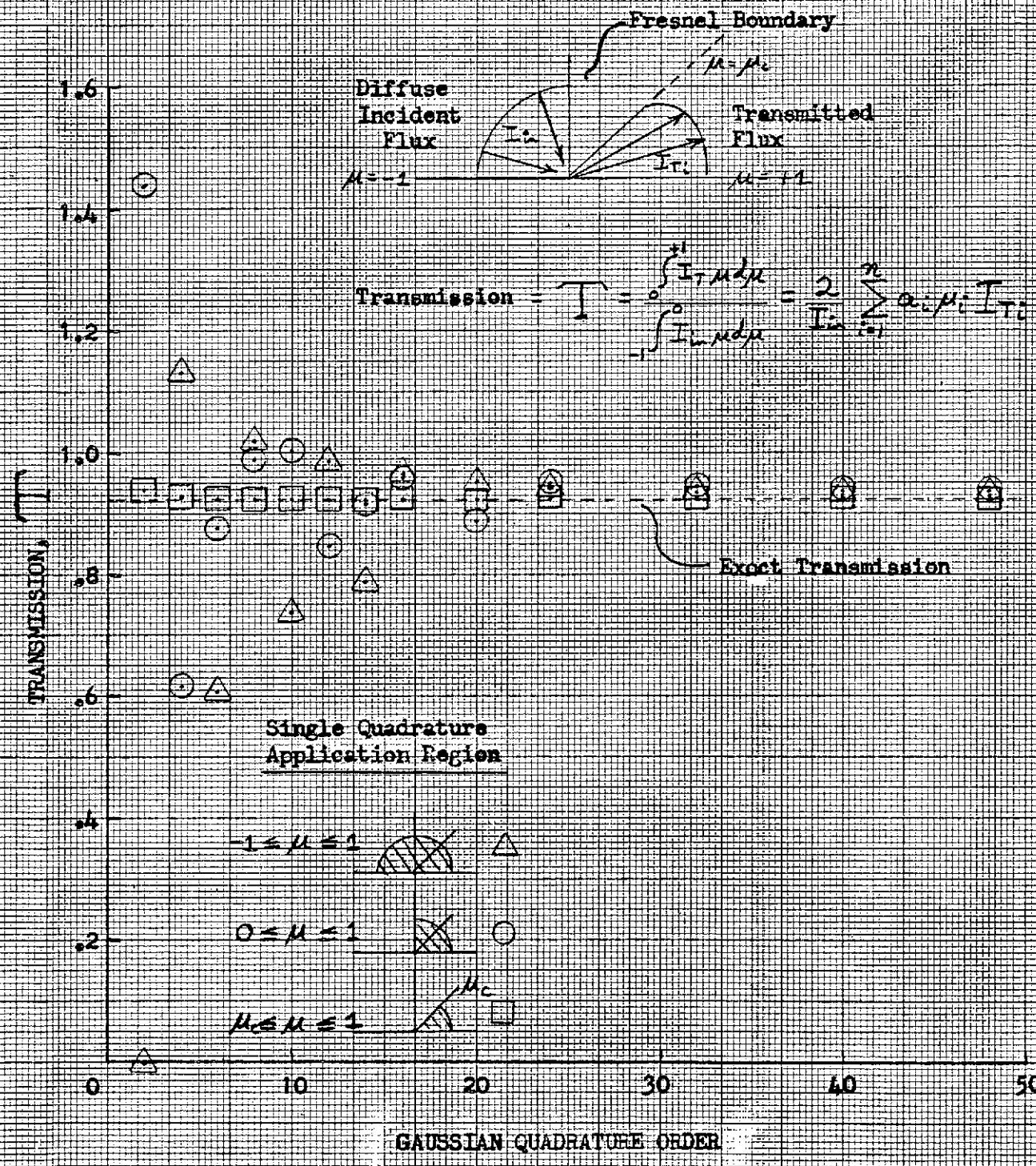
$$\gamma_0 = 1.0 \quad X = 0$$

$$R_B = .03$$

QUADRATURE COMBINATION	N = 1.4		N = 1.2	
	R	E(%)	R	E(%)
4/8/4	.290044	-.0807	.344580	-.1570
5/3/3/5	.290001	-.0659	.344429	-.1131
5/6/5	.289466	.1187	.344042	-.0006
6/4/6	.288170	.5659	.343205	.2427
10	.220740	23.83	————	————
16	.288401	.4862	————	————
2/4/2	.290637	-.2854	.345852	-.5267
3/6/3	.290197	-.1335	.344879	-.2439
Reference Value	.289810	0	.344040	0



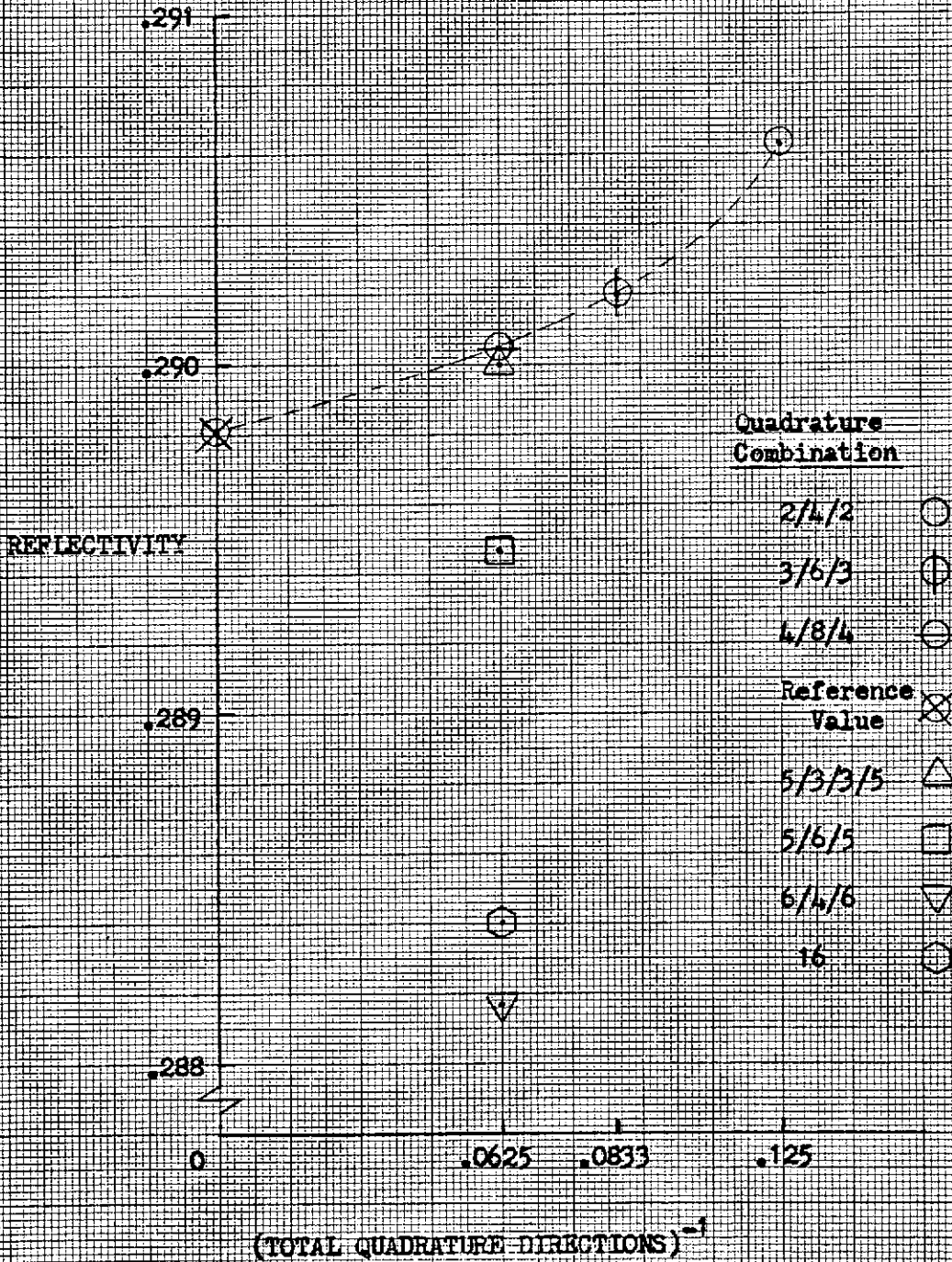
# FIGURE B1



Transmissivity of a Plane Fresnel Boundary for a Diffuse Incident Flux and Several Different Gaussian Quadratures. No Internal Radiation Incident on the Boundary. Refractive Index = 1.4.

K&E 10 X 10 TO THE CENTIMETER 46 1510  
 18 X 25 CM. KEUFFEL & ESSER CO. MADE IN U.S.A.

FIGURE B2

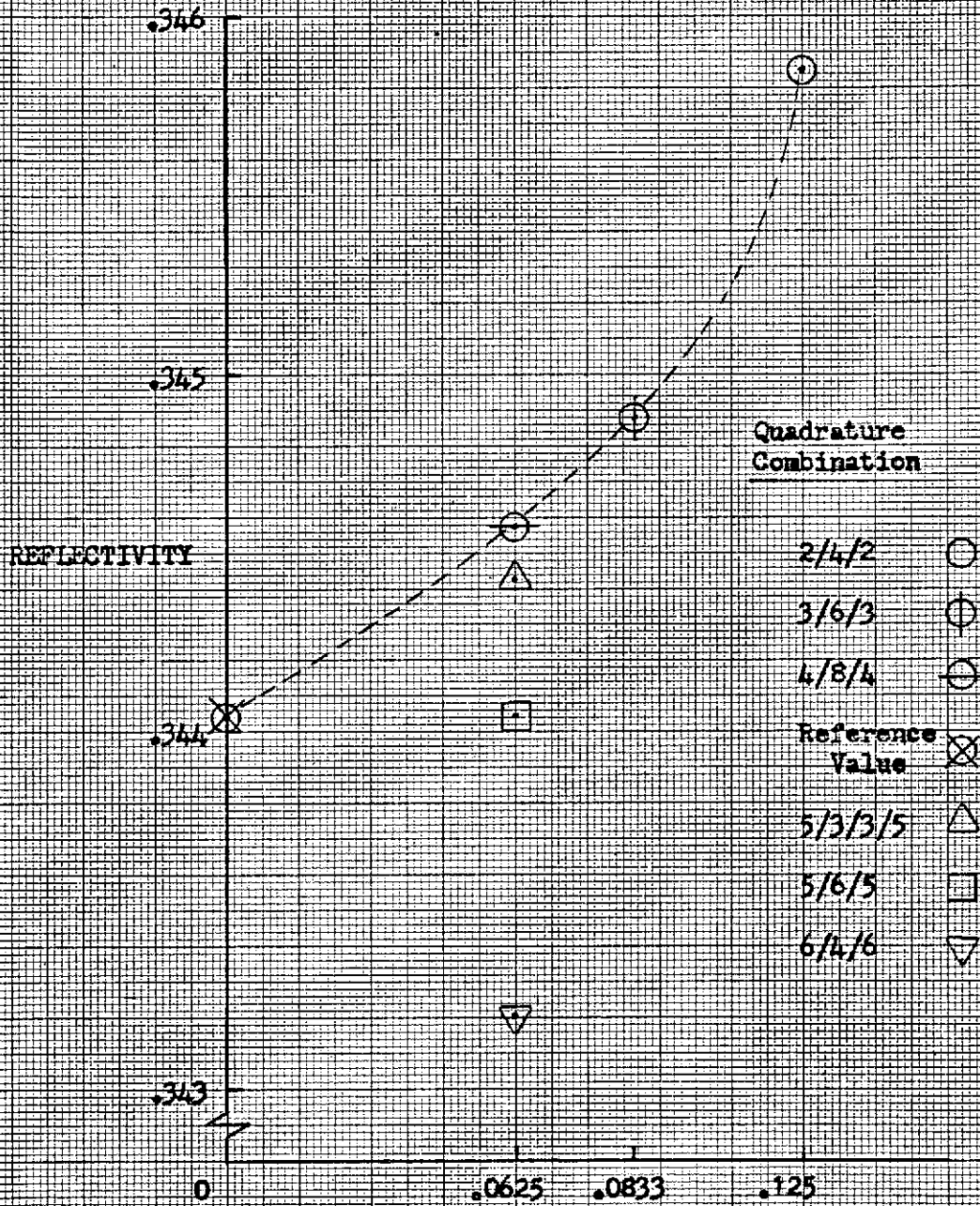


(TOTAL QUADRATURE DIRECTIONS)<sup>-1</sup>

Reflectivity Comparison for N = 1.4

$\omega = 1.0, \chi = 0, \tau_0 = 1.0, \theta^0 = K, R_D = .03$

FIGURE B.3



(TOTAL QUADRATURE DIRECTIONS)<sup>-1</sup>

Reflectivity Comparison for N = 1.2

$\omega = 1.0, \chi = 0, \tau_0 = 1.0, 0^\circ \text{K}, R_B = .03$